

# Application of Reduced Light Shift Optical Pumping Method to Chip Scale Atomic Clock

M. Zhu

Agilent Laboratories, Agilent Technologies  
5301 Stevens Creek Blvd.  
Santa Clara, CA 95051, U.S.A.

J. DeNatale

Teledyne Scientific Company  
1049 Camino Dos Rios  
Thousand Oaks, CA 91360, U.S.A.

**Abstract**—In a chip scale atomic clock (CSAC), a laser beam with a higher intensity is usually used to achieve a good contrast of the clock transition signal. Thus the light shift (AC Stark shift) is of great importance to the performance of a CSAC device. Here we apply the reduced light shift optical pumping method to a micro-machined  $^{87}\text{Rb}$  vapor cell in order to reduce the sensitivity of the measured clock frequency to various operational parameters. The preliminary result shows the improved short term stability.

## I. INTRODUCTION

It has been appreciated that the light shift (the AC Stark shift) is one of the limiting factors for the optically pumped vapor cell atomic frequency standards, both in the population-altering-pumping (PAP) configuration and in the coherent-population-trapping (CPT) configuration. Methods developed to reduce/eliminate the light shift include using a pulsed light source in PAP [1], using non-CPT-generating frequency components for compensation in CPT [2-4], and modulating the optical field intensity together with a servo system to control some operational parameters [5].

Recently, the chip-scale atomic clock (CSAC) has attracted a lot of attention [6]. In comparison with its counterpart in a conventional vapor cell based atomic clock, the alkali atom, which is confined in a smaller cell with a higher buffer gas pressure, has a shorter relaxation time in the ground state and broader optical transition linewidths. Consequently, a laser beam with a higher intensity is required to prepare the desired atomic states and to derive the clock transition signal, either in the PAP configuration or in the CPT configuration. Therefore the light shift plays an even more important role in the performance of a CSAC device.

In a CPT-based CSAC device, typically a vertical-cavity surface-emitting laser (VCSEL) is modulated at one half of the clock transition frequency. The  $\pm 1$ st order sidebands are used for generating the CPT signal while all the sidebands (including the carrier) contribute to the light shift of the observed clock transition frequency [2]. For stable operation, servo loops adjust the temperature and the current of the VCSEL in order to stabilize the VCSEL's power and

frequency. Consequently, the VCSEL's operating temperature and current change as it ages. The VCSEL's microwave modulation characteristic, which is a function of the temperature and the current of the VCSEL, changes accordingly. As a result, a frequency drift is often observed in CPT-based CSAC devices.

Here we re-visit the PAP configuration and its application to a CSAC device. In this method, the laser is not modulated at the microwave frequency so that the laser aging process has less effect on the output frequency of the device. The calculation [7], with the lowest order approximation, shows that the observed clock frequency,  $\omega_{\text{obs clock}}$ , is a function of the laser field intensity (or the laser power) and the laser frequency; but it is not influenced by the microwave power directly. Therefore our primary research goal is to reduce the light shift in a PAP-based CSAC device so that in a small range of the operational parameter space we have, at least approximately,

$$\begin{cases} \partial \omega_{\text{obs clock}} / \partial P_L = 0 \\ \partial \omega_{\text{obs clock}} / \partial \omega_L = 0 \end{cases}, \quad (1)$$

where  $P_L$  and  $\omega_L$  are the laser power and the laser frequency, respectively.

## II. THE REDUCED LIGHT SHIFT OPTICAL PUMPING METHOD

The principle of the reduced light shift optical pumping method is described elsewhere [8, 9]; a brief description is given here for completeness. Figure 1 shows a four-energy-level atom interacting with a single frequency laser field. The laser frequency,  $\omega_L$ , is tuned close to the frequencies of the transitions originating from the state  $|g2\rangle$ . First, we discuss the method to reduce the light shift of the state  $|g2\rangle$ ,  $\delta E_{g2}$ ; and later we include the effect of the light shift of the state  $|g1\rangle$ ,  $\delta E_{g1}$ . The light shift of the state  $|g2\rangle$  is given by [10]

$$\delta E_{g2} = \frac{\hbar}{4} \left\{ \frac{|\Omega_1^{g2}|^2 (\Delta_L + \omega_A)}{(\Delta_L + \omega_A)^2 + \gamma^2} + \frac{|\Omega_2^{g2}|^2 (\Delta_L - \omega_A)}{(\Delta_L - \omega_A)^2 + \gamma^2} \right\}, \quad (2)$$

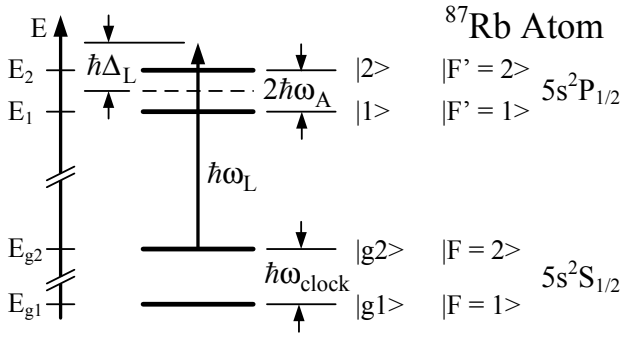


Figure 1. A system consisting of a four-energy-level atom and a single frequency laser field.  $E_i$  ( $i = g1, g2, 1$ , and  $2$ ) is the energy of the state  $|i\rangle$ . The clock transition frequency,  $\omega_{\text{clock}} \equiv (E_{g2} - E_{g1})/\hbar$ , is determined by the energy difference between the two ground states  $|g2\rangle$  and  $|g1\rangle$ . The energy difference between the two excited states  $|2\rangle$  and  $|1\rangle$  defines the parameter  $\omega_A$  using  $2\hbar\omega_A \equiv E_2 - E_1$ . The laser frequency detuning is defined as  $\Delta_L \equiv \omega_L - (E_1 + E_2 - 2E_{g2})/(2\hbar)$ , where  $\omega_L$  is the laser frequency. The energy levels related to the  $D_1$ -line in a  $^{87}\text{Rb}$  atom can be simplified to this four-energy-level structure. The corresponding states in a  $^{87}\text{Rb}$  atom are labeled on the right-hand side of the figure. See the text for discussions.

where  $\Omega_i^{g2}$  ( $i = 1, 2$ ) is the Rabi frequency for the transition between the state  $|g2\rangle$  and the state  $|i\rangle$  ( $i = 1, 2$ ),  $\Delta_L$  is the laser frequency detuning, and  $\gamma$  is the linewidth (HWHM) of the optical transition. If the conditions

$$\Delta_L = 0 \quad (3a)$$

$$|\Omega_1^{g2}| = |\Omega_2^{g2}| \quad (3b)$$

$$\gamma = \omega_A \quad (3c)$$

are met, we have

$$\begin{cases} \delta E_{g2} = 0 \\ \frac{\partial}{\partial \Delta_L} \delta E_{g2} = 0 \end{cases}, \quad (4)$$

namely, the light shift of  $|g2\rangle$  is zero and the light shift does not change with the laser frequency in the vicinity of  $\Delta_L = 0$ .

Because the condition (3b) guarantees a symmetric absorption with respect to the laser frequency detuning, the laser frequency can be stabilized to satisfy (3a) by using the conventional frequency-dither and phase-sensitive detection method. Therefore (3) is a convenient set of conditions to satisfy (4) although it is not the only one.

To apply this method to a  $^{87}\text{Rb}$  atom, we use the  $D_1$ -line for optical pumping (Fig. 1). The clock transition is defined by the sub-states  $|F = 2, m_F = 0\rangle$  and  $|F = 1, m_F = 0\rangle$  in the ground state. The laser frequency is tuned to be in resonance with the transitions from the ground state  $|F = 2\rangle$ . Although all the Zeeman sub-states in the state  $|F = 2\rangle$  contribute to the optical absorption of the laser beam inside the vapor cell, only the light shifts of the sub-states  $|F = 2, m_F = 0\rangle$  and  $|F = 1, m_F = 0\rangle$  affect the observed clock frequency. Because there are

Zeeman sub-states in each of the excited states, the condition (3b) needs to be replaced by

$$\sum_{m_F'} |\Omega_{F'=1}^{F=2, m_F=0}|^2 = \sum_{m_F'} |\Omega_{F'=2}^{F=2, m_F=0}|^2 \quad (5)$$

where the sums include all the Zeeman sub-states in the excited states  $|F' = 1\rangle$  and  $|F' = 2\rangle$ , respectively, and the small energy shifts in the Zeeman sub-states due to the bias magnetic field are ignored. Equation (5) can be realized by choosing a proper polarization of the laser field inside the vapor cell. For instance, the linear polarization

$$\hat{\mathbf{e}} = \frac{1}{\sqrt{3}}(\hat{\pi} + \hat{\sigma}_+ + \hat{\sigma}_-) \quad (6)$$

is a convenient polarization to realize the condition described by (5). The condition described by (3c) is implemented by controlling the total buffer gas pressure in the vapor cell to broaden the optical transition linewidth to the desired value.

To satisfy (1), the light shift of the state  $|F = 1, m_F = 0\rangle$  in a  $^{87}\text{Rb}$  atom needs to be included. The exact solutions similar to (3c) and (6), with the constraint (3a), are rather cumbersome. The lowest order correction, for a  $^{87}\text{Rb}$  atom, leads to

$$\Delta_L = 0 \quad (7a)$$

$$\hat{\mathbf{e}} = \frac{1}{\sqrt{3}} \left\{ \hat{\pi} + (\hat{\sigma}_+ + \hat{\sigma}_-) \left( 1 + \frac{3\omega_A}{\omega_{\text{clock}}} \right) \right\} \quad (7b)$$

$$\gamma \approx \omega_A \left( 1 - \frac{2\omega_A^2}{\omega_{\text{clock}}^2} \right). \quad (7c)$$

The reason that we choose to optically pump from the  $|F = 2\rangle$  ground state and to keep (7a) is that the absorption is symmetric with respect to laser frequency detuning due to the symmetry of the states involved. Therefore (7) can be implemented readily in practice.

### III. EXPERIMENT RESULTS

The experiment setup is similar to the one described in [8] except a micro-machined  $^{87}\text{Rb}$  vapor cell (i.d. = 2 mm, length = 2 mm) is used. A single frequency laser beam ( $\lambda = 795$  nm) is used for optical pumping. The laser beam propagates in the direction perpendicular to the DC bias magnetic field. A glass linear polarizer outside of the vapor cell entrance window defines the polarization of the laser field inside the vapor cell. The correct orientation of the glass polarizer is found by measuring the light shifts at various laser beam powers. This orientation is defined as  $0^\circ$  in the rest of the measurements.

Fig. 2 shows the relative clock frequency versus the laser frequency detuning at four laser beam power settings. In this measurement, a reference laser is used. The frequency of the reference laser is locked to a  $^{85}\text{Rb}$  transition ( $|F = 3\rangle \rightarrow |F' = 3\rangle$ ) in a rubidium cell without buffer gas using the FM saturation spectroscopy method. A microwave frequency synthesizer controls the offset frequency between the two

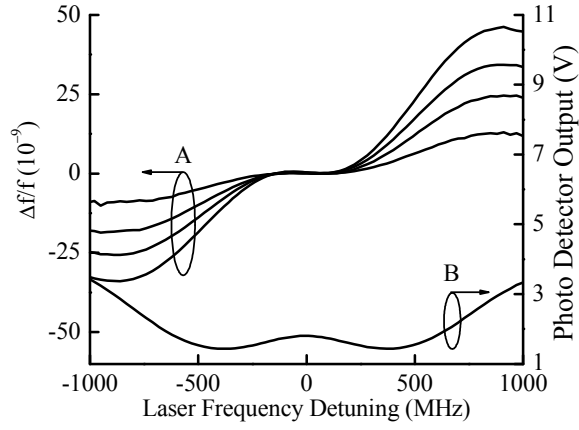


Figure 2. A: The measured relative clock frequency vs. the laser frequency detuning at four laser beam power settings (3.75  $\mu\text{W}$ , 7.50  $\mu\text{W}$ , 11.25  $\mu\text{W}$ , and 15.00  $\mu\text{W}$ ). The glass polarizer is set at  $0^\circ$  as defined in the text. B: The DC output voltage of the photo detector, which measures the transmitted laser beam. See the text for details.

lasers. The measurement shows that in the vicinity of zero detuning, the clock frequency is insensitive to a change in the laser frequency. The small negative slope of the curves near zero detuning is attributed to the fact that the total buffer gas pressure in the vapor cell is slightly lower than the ideal value. Fig. 2 also shows the DC output of the photo detector. The local absorption minimum is located at zero detuning, which is used to stabilize the frequency of the optical pumping laser in all of the following measurements in this experiment.

Fig. 3 shows the measured relative clock frequency versus the laser beam power at three glass polarizer orientations. It shows that when the glass polarizer is oriented at  $0^\circ$ , the clock frequency is indeed insensitive to the change of the laser beam power. This means the total light shift is cancelled by choosing the polarization correctly according to (7b).

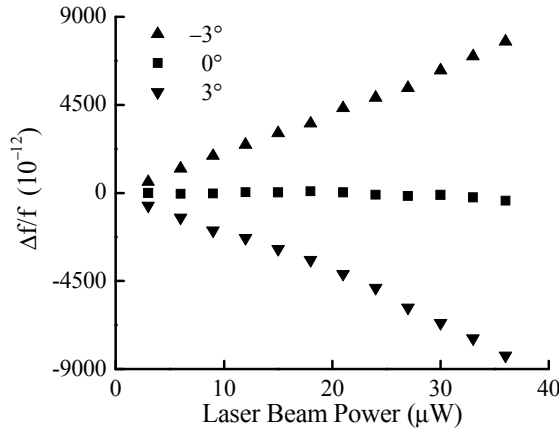


Figure 3. The relative clock frequency measured in a micro-machined  $^{87}\text{Rb}$  vapor cell (i.d. = 2 mm, length = 2 mm). The angles indicate the orientations of the glass linear polarizer with respect to the nominal zero light shift polarization. See the text for details.

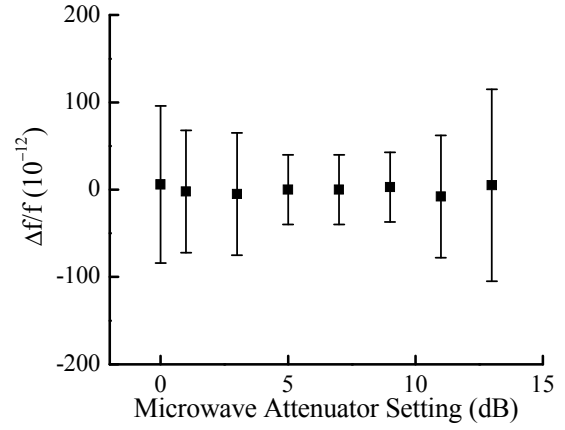


Figure 4. The measured relative clock frequency vs. the microwave attenuator settings. The glass polarizer is set at  $0^\circ$  as defined in the text. See the text for details.

To test the dependence of the clock frequency on the microwave power, a microwave attenuator is used to control the microwave power delivered to the vapor cell assembly. Fig. 4 shows the relative clock frequency at various settings of the microwave attenuator. The measurement agrees with the calculation [7].

Fig. 5 shows the Allan deviation of the experiment. The short term stability is improved, especially in the range where the averaging time is longer than 1000 s, in comparison with a CPT-based system using a vapor cell with the same size. It is noteworthy that neither the laser power nor the microwave power is stabilized in this preliminary experiment.

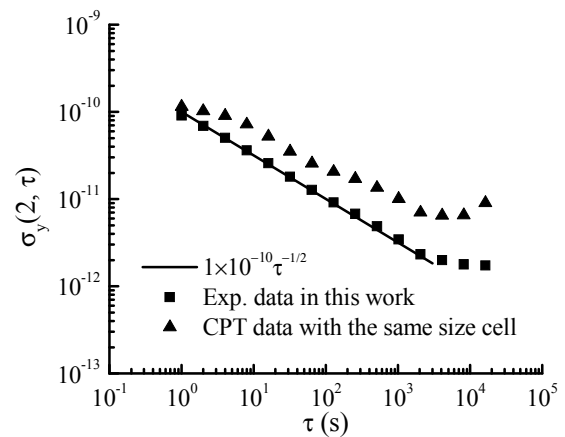


Figure 5. The Allan deviations measured with a micro-machined  $^{87}\text{Rb}$  vapor cell (i.d. = 2 mm, length = 2 mm). The glass polarizer is set at  $0^\circ$  as defined in the text. The CPT data with the same size cell is included for comparison. See the text for details.

#### IV. SUMMARY

We apply an optical pumping method with reduced light shift to a micro-machined vapor cell. Using this method we show that the clock frequency is less sensitive to the laser frequency detuning, the laser power, and the microwave power. We also show the improved Allan deviation in comparison with a CPT-based device using a vapor cell that has the same dimensions. This method offers an alternative realization of the chip-scale atomic clock. Improved performance of the CSAC device using this method is expected.

#### ACKNOWLEDGMENT

The authors thank Frank Lucia for making various parts in this work. The authors are grateful to Robert Borwick and Alan Sailer for preparing the Rb vapor cells used in this work. The authors thank Curt Flory and Jim Johnson for reading this manuscript carefully and providing many suggestions.

#### REFERENCES

- [1] See, for example, A. Godone, F. Levi, S. Micalizio, E. K. Bertacco, and C. E. Calosso, *IEEE Trans. Instrum. Meas.*, 56, 378, (2007).
- [2] M. Zhu and L. S. Cutler, *Proceedings of the 32nd Annual Precise Time and Time Interval Systems and Applications Meeting*, p. 311, (2000).
- [3] M. Zhu and L. S. Cutler, *US Patent* 6,201,821 (2001).
- [4] M. Zhu and L. S. Cutler, *US Patent* 6,363,091 (2002).
- [5] See, for example, V. Shah, V. Gerginov, P. D. D. Schwindt, S. Knappe, L. Hollberg, J. Kitching, *Appl. Phys. Lett.*, 89, 151124 (2006).
- [6] See, for example, the website of the Microsystems Technology Office in the Defense Advanced Research Projects Agency, <http://www.darpa.mil/MTO/programs/csac/>.
- [7] M. Zhu, unpublished.
- [8] M. Zhu, *Proceedings of Joint Conference of 2007 IEEE International Frequency Control Symposium and 21<sup>st</sup> European Frequency and Time Forum*, p. 1334 (2007).
- [9] M. Zhu, U.S. patent pending.
- [10] See, for example, L. Schiff, *Quantum Mechanics*, McGraw-Hill, (1968).